RAA 2021 Vol. **21** No. **12**, 297(8pp) doi: 10.1088/1674-4527/ac2942

http://www.raa-journal.org *http://iopscience.iop.org/raa*

***R**esearch in*
***A**stronomy and*
***A**strophysics*

Thermodynamic model of the activity of the comet 103P/Hartley ⋆

Marcin Wesołowski

College of Natural Sciences, Institute of Physics, University of Rzeszów, Pigonia 1 Street, 35-310 Rzeszów, Poland; *mwesolowski@ur.edu.pl*

Received 2021 July 31; accepted 2021 September 18

Abstract The paper presents three processes related to the dynamics of cometary particles. The following thermodynamic mechanisms were taken into account: quiet sublimation, emission of cometary matter via jet and migration of particles on the surface of the comet 103P/Hartley. Based on the first two mechanisms, the maximum particle size that can be lifted into the coma was determined. Additionally, in the case of a jet, the angle at which it is emitted from inside the cometary nucleus was determined. However, in the case of migration, the maximum width of individual belts within which a given particle can move was determined. In the context of the discussed mechanisms related to the activity of comet 103P/Hartley, the coefficient of friction and the structure of the solid or porous particles are of key importance.

Key words: comets: general — comets: individual: 103P/Hartley

1 INTRODUCTION

The comet 103P/Hartley (hereafter 103P) is a small comet that belongs to the group of short-period comets. It was discovered in 1986 by Malcolm Hartley using the Schmidt Telescope Unit in the Siding Spring Observatory. The comet's orbit has the shape of an ellipse with the eccentricity $e = 0.69$. The comet's perihelion is relatively close to Earth ($q = 1.06$ au) and therefore belongs to the group of Near-Earth Objects (NEOs). Note that asteroids, comets, and meteoroids are also included in this group. By convention, a Solar System body is an NEO if its closest approach to the Sun (perihelion) is less than 1.3 au. The comet's aphelion is 5.87 au and it has an orbital period around the Sun of 6.46 yr. Moreover, the orbit of comet 103P is inclined with respect to the plane of the ecliptic at i = 13.6°. Based on the above orbital parameters, it can easily be shown that the Tisserand parameter for comet 103P is $T_{\rm J}$ = 2.644. This means that comet 103P belongs to the Jupiter family of comets. Additionally, we emphasize clearly that in the case of this comet family, the Tisserand parameter satisfies the following relationship: $2 \leq T_{\rm J} \leq 3$ (Levison & Duncan 1994; Gronkowski & Wesołowski 2015a; Wesołowski et al. 2020c). Note that, based on statistical analysis, Belton proposed that comets belonging to the Jupiter family satisfy the following two relationships: $2.4 \leq T_{\rm J} \leq 3.1$ and $0° \leq i \leq 31°$ (Belton 2014; Belton 2015).

The nucleus of comet 103P has a prolate shape and dimensions on the order of 1.6 × 2.2 km, and it rotates in 18.1 h. Detailed studies of this comet were carried out in late 2010 during the EPOXI space mission. The obtained results allowed for the development of a gas eruption map, observation of the inner part of the coma, changes in the brightness and temperature profile on the surface of the nucleus, and analysis of the chemical composition. It was a surprise for astronomers all over the world that cometary activity was controlled by sublimation of carbon dioxide so close to the Sun (q = 1.06 au). In addition, the cometary nucleus was surrounded by a cloud of water ice fragments up to 25 cm in size, which was ejected from the core by numerous jets (A'Hearn et al. 2011; Farnham et al. 2011; Feaga et al. 2011; Hermalyn et al. 2011; Schultz et al. 2011; Sunshine et al. 2011). Jets have also been observed in other comets including 19P/Borelly, 29P/Schwassmann-Wachmann and 67P/Churyumov-Gerasimenko.

This paper aims to present the mechanisms related to the thermodynamic emission of cometary matter. This paper should be seen as an extension and improvement of previous papers (Gronkowski & Wesołowski 2015b, 2017; Wesołowski et al. 2019, 2020c; Wesołowski 2020b). Based on the considerations presented in this paper, we can distinguish two specific goals. The first is to determine the size of the particles that can be lifted into the coma

⋆ University of Rzeszów, Poland.

in the case of quiet sublimation and jet. The second goal is to determine the width of individual migration belts depending on the particle size and the coefficient of friction. Moreover, in both of these cases, the structure of a given solid or porous particle is of key importance. Let us add that the migration of particles is an important stage in the formation of individual structures (e.g. cliffs) on the surface of a comet's nucleus. The direct evidence for this statement is the results obtained during the Rosetta mission.

2 THERMODYNAMIC MECHANISMS - BASIC INFORMATION

In the considerations presented below, the key parameter is to determine the temperature profile. Therefore, at this point, we rely on the energy balance equation. The second important step in the calculations is to determine the speed of sublimating cometary gas molecules and their sublimation rate. A detailed discussion of these thermodynamic parameters has been presented in many papers (e.g. Keller 1990; Enzian et al. 1997; Capria et al. 2003; Marboeuf et al. 2012; Gronkowski & Wesołowski 2015a; Skorov et al. 2017; Wesołowski et al. 2019, 2020a,b,c; Wesołowski 2020a, 2021a,b,c,d). Therefore, the above equations are presented only in the form of the system of Equations (1)–(3).

$$\frac{S_{\odot}}{d^2}(1-A_{\mathrm{N}})\cos\varphi = \epsilon\sigma T^4 + h(\psi)K(T)\frac{\Delta T}{\Delta x} + \frac{\dot{Z}L(T)}{N_{\mathrm{A}}}. \tag{1}$$

$$v_{\mathrm{th}} = \frac{4}{\pi}\sqrt{\frac{\pi k_{\mathrm{B}}T}{2m_{\mathrm{g}}}}, \tag{2}$$

$$\dot{Z} = \frac{A_{\mathrm{CO_2}}\cdot\exp(-B_{\mathrm{CO_2}}\cdot T^{-1})}{\sqrt{2\pi k_{\mathrm{B}}Tm_{\mathrm{g}}}}, \tag{3}$$

A detailed explanation of the individual symbols in Equations (1)–(3) can be found in Wesołowski & Gronkowski (2018a,b).

2.1 Emission of Cometary Matter

At the very beginning, it should be noted that cometary particles that are on the surface of a comet's nucleus are subject to the following forces: gravitation of the nucleus, drag force coming from the molecules of sublimating ices, centrifugal force related to the rotation of the nucleus, radiation force related to electromagnetic solar radiation, solar tidal force which is a consequence of the orbital the motion of the comet, Coriolis force and rocket force. Note that in the context of the emission of particles into space, only the first three forces play a key role (Gronkowski & Wesołowski 2015b, 2017; Wesołowski 2020b). When considering the actual shape of a cometary nucleus, the equation of particle motion must contain non-uniform gravitational acceleration, which was calculated taking into account the irregular shape of comet 103P (Thomas et al. 2013). Therefore, the equation for the motion of such a particle can be written as follows

$$m_{\mathrm{dust}}\frac{\mathrm{d}v_{\mathrm{dust}}}{\mathrm{d}t} = \frac{1}{2}C_{\mathrm{D}}\pi a_{\mathrm{dust}}^2\left(v_{\mathrm{g}}-v_{\mathrm{dust}}\right)^2\varrho_{\mathrm{g}} + m_{\mathrm{dust}}\omega^2 a\cos(\mathrm{t})\sin(\beta) - g_{\mathrm{c}}m_{\mathrm{dust}}. \tag{4}$$

The first term on the right side of this equation stands for the drag force coming from the comet's gases, the

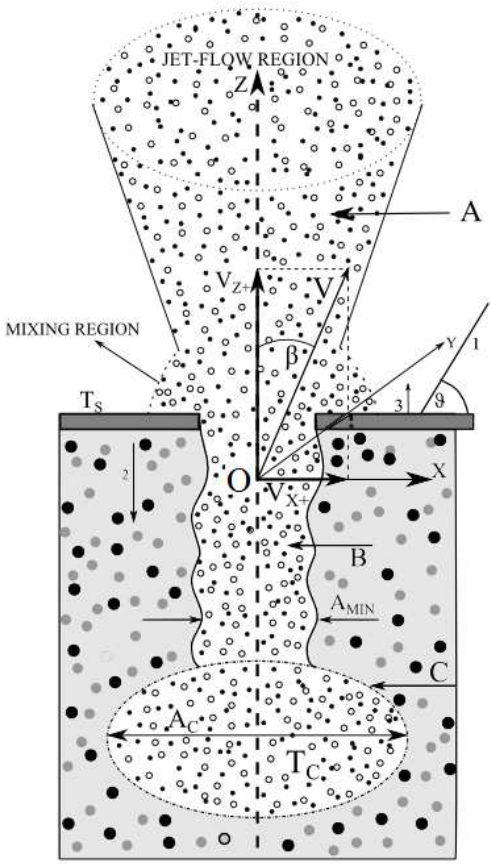

Fig. 1 A cross-section through the surface layer of a cometary nucleus in the vicinity of a geyser. The following notations are adopted: 1 - solar radiation that reaches the cometary nucleus, 2 - heat conducted to the cavity, 3 - re-radiated energy, A - a geyser's jet, B - the channel of a geyser, C - a cavity, T_{C} - temperature in the cavity and T_{S} temperature on the surface of the cometary nucleus. Note that the geyser model should take into account gas flow and mixing (Belton 2010). The outlet from the geyser, i.e. the angle at which the jet is emitted, is marked as β', while its value is determined by two components of the velocity of gas molecules $v_{\mathrm{x}+}$ and $v_{\mathrm{z}+}$ emitted along the OX_+ and OZ_+ axes respectively.

Table 1 Values of the Physical Cometary Parameters Used in the Numerical Calculations and Simulations

Parameter	Value(s)	Reference
Mean radius of the cometary nucleus (km)	$R_{\rm N}$=0.58±0.018	Thomas et al. (2013)
Heliocentric distance (au)	d=1.06	Value adopted
Gravitional acceleration (cm s^{-2})	g=0.0019-0.0044	Thomas et al. (2013)
Mean depth of depression (m)	h=10	Value adopted
Density of cometary nucleus (kg m^{-3})	$\rho_{\rm N}$=300	Thomas et al. (2013)
Albedo of the cometary nucleus (-)	$A_{\rm N}$=0.028	Lisse et al. (2009)
Emissivity (-)	ϵ = 0.9	Wesołowski et al. (2019)
Density of dust particles (kg m^{-3})	$\rho_{\rm c}$=3000	Fulle et al. (2016)
Hertz factor (-)	h(ψ) = 0.01	Kossacki & Szutowicz (2013)
Porosity of nucleus (-)	ψ = 0.65	Gronkowski & Wesołowski (2015a)
The solar constant (for d=1 au) (W m^{-2})	$S_{\odot}$=1360.8±0.5	Kopp & Lean (2011)
Constant A_{CO_2} for carbon dioxide (Pa)	A_{CO_2} = 107.9 × 10^{10}	Prialnik (2006)
Constant B_{CO_2} for carbon dioxide (K)	B_{CO_2} = 3148.0	Prialnik (2006)
Latent heat of carbon dioxide sublimation (J kg^{-1})	L(T)$_{CO_2}$=0.594 × 10^6	Prialnik (2006)

second one represents the centrifugal force related to the rotation of the comet's nucleus and the last is the gravitation of the cometary nucleus. The symbol β denotes the cometocentric latitude, $m_{\rm dust}$ is the mass of the considered particles, $C_{\rm D}$ is the drag factor that characterizes force exerted on dust by gas, the symbol $a_{\rm dust}$ signifies the radius of a moving particle, $v_{\rm g}$ is the gas flow velocity, $v_{\rm dust}$ is the velocity of particles, $\varrho_{\rm g}$ is the density of cometary gas, ω is the angular velocity of the cometary nucleus and $g_{\rm c}$ is the gravitational acceleration from the cometary nucleus.

Assuming in Equation (4) the condition that $\mathrm{d}_{\rm dust}/\mathrm{d}t \geq 0$, we can determine the maximum radius of the emitted particle into a coma as

$$a_{\rm dust} = \frac{3C_{\rm D}v_{\rm g}^2\varrho_{\rm g}}{8\varrho_{\rm c}(g_{\rm c} - \frac{4\pi^2 a\cos(\mathrm{t})\sin(\beta)}{P_{\rm s}^2})}. \tag{5}$$

In Equation (4), the individual symbols mean: $\varrho_{\rm c}$ denotes the density of large cometary particles and $P_{\rm s}$ is the rotational period of the cometary nucleus. Note that based on Equation (4), one can consider two models: without centrifugal force (very slowly rotating nucleus - $P_{\rm s} \to \infty$), and with centrifugal force, whose rotation period is $P_{\rm s}$ = 18.1 h.

Analyzing the results of space probes, starting from the mission-related to comet 1P/Halley, we can see that one of the characteristic manifestations of comet activity is numerous collimated streams of gas jets. These streams are emitted into space through cracks, fissures and cryovolcanoes (Yelle et al. 2004; Ipatov & A'Hearn 2011; Combi et al. 2012; Ipatov 2012; Vincent et al. 2015; Groussin et al. 2015; Preusker et al. 2015; Sierks et al. 2015; Tubiana et al. 2015; Jorda et al. 2016; Gicquel et al. 2017). A consequence of the jets is the emission of dust by the collimated gas stream compared to the emission from the cometary surface. By proceeding in the same way as in the case of quiet sublimation, it can be shown that the maximum particle radius emitted by jets is given by a relationship

$$a_{\rm dust,jet} = \frac{3C_{\rm D}v_{\rm gey}(1-\alpha)}{8\varrho_{\rm c}(g_{\rm c} - \frac{4\pi a\cos(\mathrm{t})\sin(\beta)}{P^2})\alpha L(T)}h(\psi)K(T)\frac{\Delta T}{\Delta x}. \tag{6}$$

A detailed description of Equation (6) can be found in Wesołowski et al. (2020c).

From the observations of comets and jets, in particular, it is clear that the value of the gas stream deflection angle is on the order of several degrees. The angle of deflection of the gas stream can be estimated from the jet related morphology. The key issue is to adopt an appropriate thermodynamic model related to the speed of sublimating gas molecules.

Assuming that the jet has a simple cylindrical shape, the movement of the gas in the jet does not have a Maxwellian distribution in three dimensions due to the strong acceleration along the OZ axis (Fig. 1). Then the movement of this gas can be described using the Maxwellian distribution function only along the OX axis and OY axis. In other words, only the two-dimensional (2D) Maxwellian distribution characterizes gas in the jet. However, the shape of a jet determines the movement of gas molecules only in the positive direction of semi-axis OX$^+$ (or only in the negative direction of semi-axis OX$^-$) if we look along the OY axis (see Fig. 1).

Then the deviation angle β' is a function of the average value of the component velocity of gas molecules $v_{\rm x^+}$ along semi-axis OX+, and the average value of the component velocity of gas molecules $v_{\rm z^+}$ along semi-axis OZ$_+$. It is worth noting that we can obtain the deviation angle of a jet β from the following simple formula

$$\tan(\beta') = \frac{v_{\rm x^+}}{v_{\rm z^+}}. \tag{7}$$

The velocity component $v_{\rm x^+}$ occurring in Equation (7) can be calculated from the following formula

$$v_{\rm x^+} = \int_0^{+\infty}\int_{-\infty}^{+\infty} f(v_{\rm x}, v_{\rm y})\mathrm{d}v_{\rm x}\mathrm{d}v_{\rm y}, \tag{8}$$

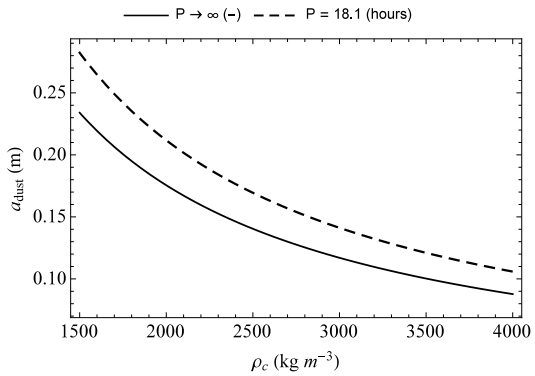

Fig. 2 The maximum radius of comet particles ($a_{\rm dust}$) that can be lifted from the surface of comet 103P as a function of particle density ($\varrho_{\rm c}$). The calculations assume that the comet is at the perihelion of its orbit and its activity is controlled by carbon dioxide sublimation. In addition, the calculations feature two models, slowly rotating and rotating with a spin period of 18.1 h.

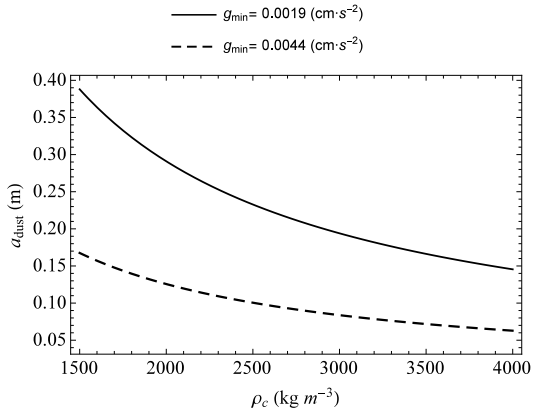

Fig. 3 The same as in Fig. 2, but the calculations include the influence of two extreme values of gravitational acceleration. The presented calculations refer to the slowly rotating model.

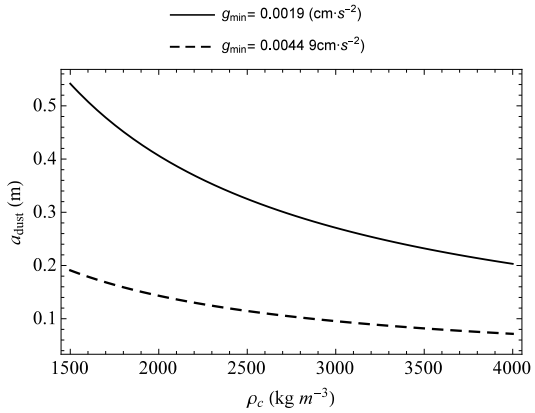

Fig. 4 The same as Fig. 3, but calculations are based on a rotating model with a spin period of 18.1 h.

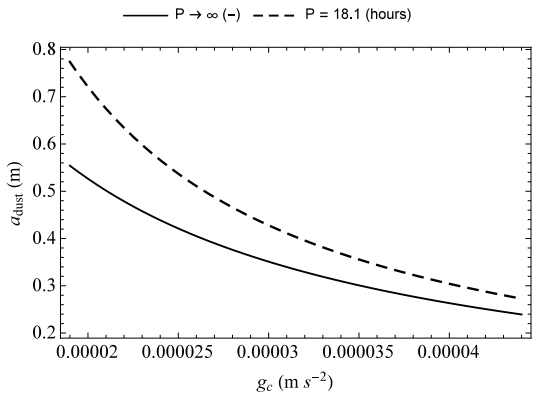

Fig. 5 The maximum radius of the cometary particles (a $_{\rm dust}$) that can be lifted from the surface of comet 103P as a function of gravitational acceleration. As with Fig. 1, two models, slowly spinning and rotating with a spin period of 18.1 h, were considered. The presented calculations concern a porous particle with a density of 1050 kg m^{-3}.

where $f(v_{\rm x}, v_{\rm y})$ is the Maxwellian 2D gas distribution function. It is given as follows

$$f(v_{\rm x}, v_{\rm y}) = \left(\frac{m_{\rm g}}{2\pi k_{\rm B} T_{\rm s}}\right) \exp\left(\frac{-m_{\rm g}(v_{\rm x}^2 + v_{\rm y}^2)}{2k_{\rm B} T_{\rm s}}\right). \quad (9)$$

In this expression, $m_{\rm g}$ and $T_{\rm s}$ stand for the mass of gas molecules and temperature respectively. The second component of the velocity $v_{\rm z+}$ appearing in Equation (7) is equal to the velocity of the gas stream in the geyser channel. In the case of a jet whose activity is controlled by the emission of CO, $\beta' \approx 31.096°$ and for CO_2 the angle $\beta' \approx 29.422°$. Note that for water ice the adiabatic exponent is the same as for CO_2 ice, so the β angle is 29.422°. Let us add that the obtained values of the β' angle are consistent with contemporary observations of the cometary jets (see Gicquel et al. 2017). Of course, we must bear in mind that in reality, the shape of a jet depends on the geometry of the orifice of the geyser. It depends in particular on the shape of the end part of the stream channel.

2.2 Dust Migration

The considerations presented in Section 2.1 concern the emission of comet material from the surface of the nucleus as a result of quiet sublimation and from the interior of the nucleus through a jet. In these two cases, the dimensions of the particles that are emitted into the coma significantly depend on the sublimation rate and the gas stream flowing through the geyser. Another mechanism related to the movement of particles along the surface of a spinning comet nucleus is their migration. This phenomenon is related to the movement of particles, i.e. a change in

Table 2 The width of the migration belts for particles depending on the coefficient of friction. The calculations correspond to the results displayed in Fig. 10.

	$\Delta\beta(^\circ)$			
	$a_{\rm dust}$ (cm)			
$\mu_{\rm s}$ (-)	14.18	14.22	14.35	14.50
0.3	76.49	75.85	73.78	71.41
0.5	68.01	66.91	62.24	58.90
0.7	60.24	58.61	53.07	46.11
0.9	53.33	51.12	43.31	32.35

Table 3 The width of the migration belts for particles depending on the coefficient of friction. The calculations correspond to the results displayed in Fig. 11.

	$\Delta\beta(^\circ)$			
	$a_{\rm dust}$ (cm)			
$\mu_{\rm s}$ (-)	40.50	40.60	40.90	51.50
0.3	76.57	76.01	74.82	71.01
0.5	68.14	67.18	64.23	58.17
0.7	60.44	59.02	54.61	44.88
0.9	53.62	51.68	45.52	30.18

their cometocentric latitude. The direct cause of particle migration is the sublimation of given ice and an increase in the rotation rate of the comet nucleus.

In the context of particle migration, particle size is a key factor. When considering the possibility of migration of a given particle along the surface of the nucleus, the same forces as in the case of silent sublimation and the forces related to the substrate reaction should be taken into account: normal reaction force and friction force. Note that Wesołowski et al. (2019) present a detailed discussion of dust migration depending on the adopted nucleus shape. In this article, however, we want to study the migration of dust along the surface of comet 103P. Thus, the condition of particle migration, in this case, takes the form

$$f(\beta) = \frac{\frac{-4\pi^2}{P^2}a\cos(t)\cos(\beta)}{g_{\rm c}\sin(\beta-\gamma) - \frac{3C_{\rm D}v_{\rm g}^2\varrho_{\rm g}}{8\varrho_{\rm c}a_{\rm gr}} - \frac{4\pi^2}{P^2}a\cos(t)\sin(\beta)}. \quad (10)$$

Note that in Equation (10) there is an $a_{\rm gr}$ parameter which determines the size of a particle that can migrate across the cometary surface. The individual symbols used in Equation (10) have the same meanings as above. In the context of the above assumptions, let us note that the motion of a given particle is possible when the following condition is met: $\mu \leq f(\phi)$, where μ means the coefficient of friction and $f(\phi)$ is the migration coefficient.

3 RESULT

The paper presents selected thermodynamic mechanisms responsible for the emission and migration of cometary particles. Appropriate physical constants were applied in the numerical calculations, which are presented in Table 1. In the first case, we consider the emission of cometary particles from the nucleus surface as a result of the quiet sublimation of CO_2 ice. In this case, the calculations performed relate to two types of agglomerates with a solid or porous structure (Figs. 2–5). For porous agglomerates, it was assumed that the porosity coefficient is $\psi = 0.65$ was taken into account (Gronkowski & Wesołowski 2015a). Then the density of the porous agglomerate assumes the value of 1050 kg m^{-3}.

In the second case, the emission of cometary particles via the jet was considered (Figs. 6–9). In both of these cases, a wide range of particle densities and two extreme values of gravitational acceleration were taken into account (see Thomas et al. 2013). Additionally, two slow-rotating models were included in the calculations: ($P_{\rm s}$ $\rightarrow \infty$) and rotating with a spin period equal to $P_{\rm s}$=18.1 h. In addition, in the case of the jet, based on the Maxwellian velocity distribution, the angle of the jet at which it is emitted from the inside of the cometary nucleus was estimated.

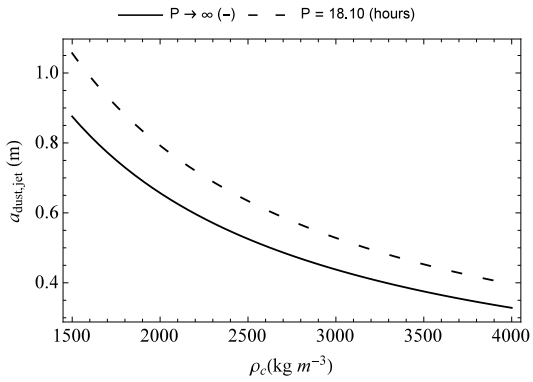

Fig. 6 The same as in Fig. 2, but particle emission occurs through gas stream emitted by the jet.

In the third case, the migration of particles on the surface of the spinning comet nucleus was considered. In the context of analyzing the results of particle migration, the radius and density of the particle under consideration are key factors. The results of migration of individual cometary particles together with the adopted value of the coefficient of friction determine the width of the individual

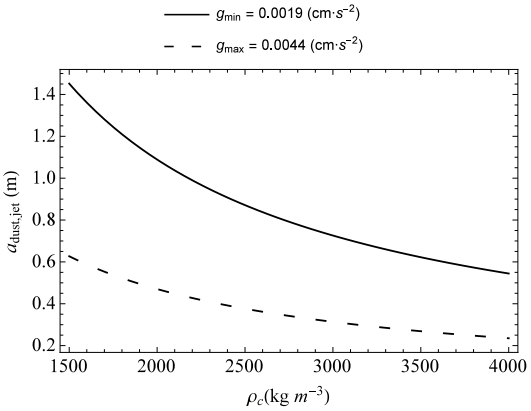

Fig. 7 The same as in Fig. 3, but particle emission occurs through the gas stream emitted by the jet.

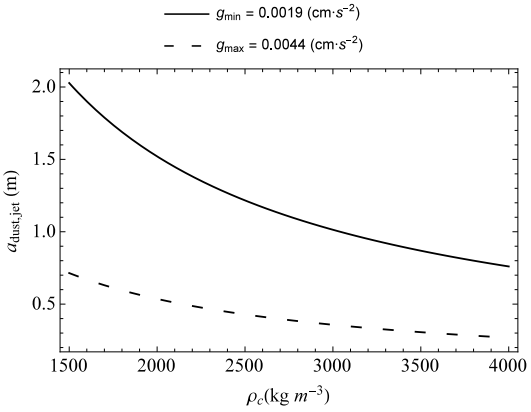

Fig. 8 The same as in Fig. 4, but particle emission occurs through the gas stream emitted by the jet.

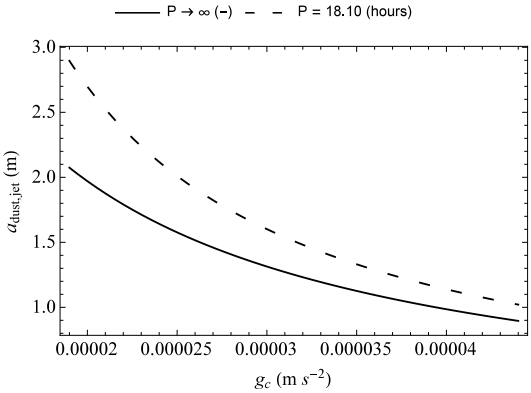

Fig. 9 The same as in Fig. 5, but particle emission occurs through the gas stream emitted by the jet.

stripes (Figs. 10–11). As in the first two mechanisms, it was assumed that the migrating particle has a solid or porous structure. Tables 2–3 display the widths of the migration belts for particles with a certain radius. Note that

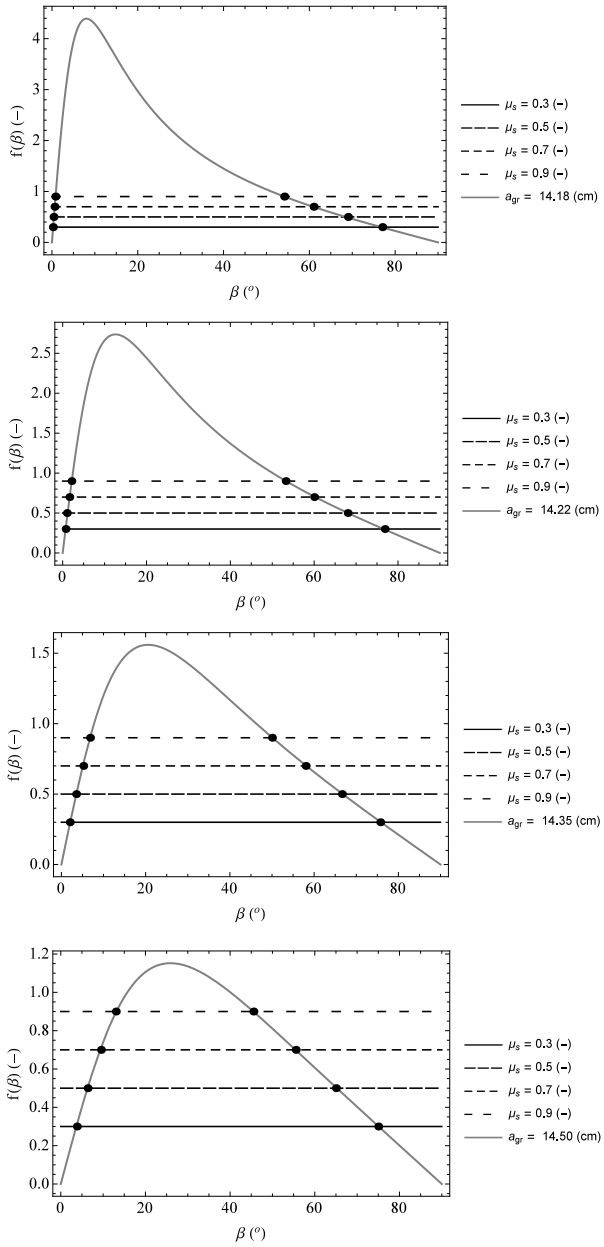

Fig. 10 The distribution of the migration coefficient depending on the cometocentric latitude and the assumed four values of coefficient of friction. The calculations take into account that the particle has a solid structure and its density is 3000 kg m^{-3}.

the values of the width of the migration belts for a given coefficient of friction are comparable with each other. Note also that these results determine the maximum width of these stripes. It is also obvious that a given particle can cross a smaller cometocentric latitude. This may be due to the particle being stuck in a pit or cavity or on a cliff. In this case, the detailed surface structure of the cometary nucleus is crucial.

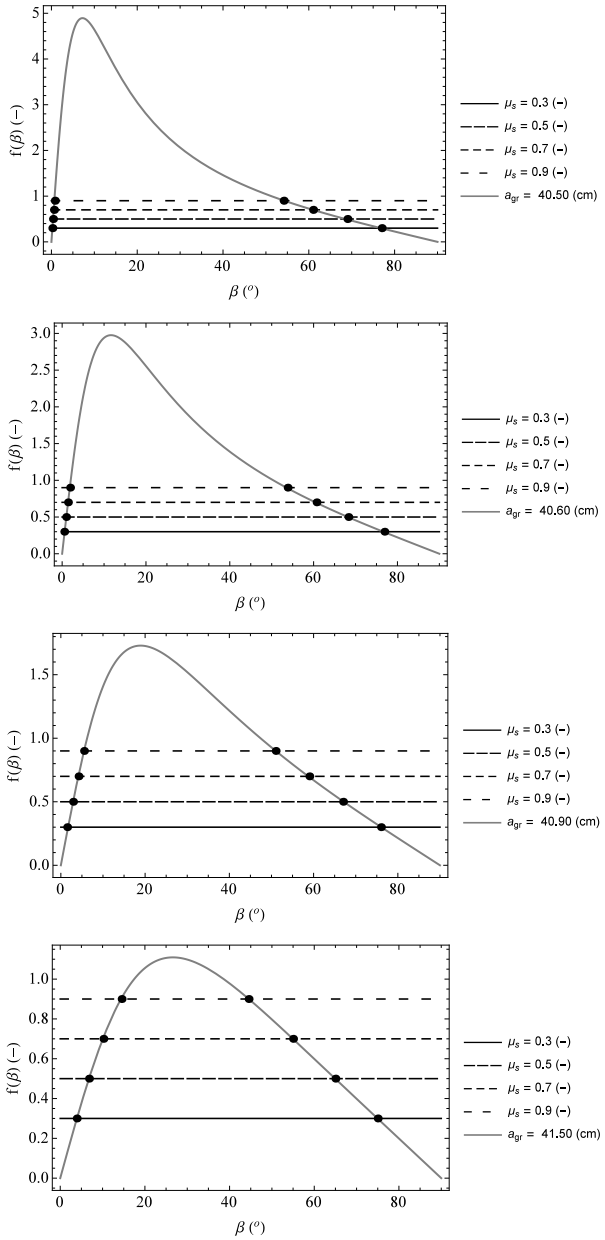

Fig. 11 The same as in Fig. 10, but the calculations refer to a porous particle with a density of 1050 kg m^{-3}.

The calculation results presented below concern the perihelion of the orbit of comet 103P.

4 SUMMARY AND CONCLUSIONS

The research presented in this paper concerns the determination of the maximum size of particles that can be lifted into a coma by quiet sublimation or jet. This approach was a consequence of determining the upper limit of the particle radius which under given physical conditions may leave the nucleus or change its original position. Therefore, the presented calculation results refer to the maximum temperature and sublimation rate. The measure of the radius of the particle lifted into the coma is the sublimation rate of the cometary ice, the particle density, the local gravitational acceleration and the size of the nucleus. Also, in the context of a particle rising or falling at a new location, the structure of the particle plays a key role.

Note that the dimensions of the particles that are emitted into the coma are greater with rhinestones than with silent sublimation. Additionally, the rotation of the comet nucleus increases the particle size by up to 20%. Moreover, the emission of gas and dust particles through the stream and sublimation from the inner walls of the geyser may contribute to the formation of a local depression (Leliwa-Kopystynski 2018).

Considering the migration of dust along the surface of the nucleus, it should be clearly emphasized that this process is initiated by the sublimation of given ice and changes in the rate of rotation of the cometary nucleus. Based on these considerations, we can formulate two important conclusions. First, this mechanism takes place over a longer time scale (e.g. several orbital periods), which may contribute to a change in the topography of the nucleus surface by initiating local cometary avalanches (Steckloff & Melosh 2016; Pajola et al. 2017; Wesołowski et al. 2020a). On the other hand, dust migration is responsible for changing the position of particles on the surface of the nucleus. This, in turn, may lead to the formation of a sinkhole as a result of excessive loading of the upper part of the cavity with comet material (dust and rock crumbs). If we assume that the cavity was at least partially filled with gas and dust, then particle migration may be responsible for the formation of jets. On the other hand, if the cavity was a space, then particle migration is responsible for the formation of pits on the surface of the cometary nucleus.

References

A'Hearn, M. F., Belton, M. J. S., Delamere, W. A., et al. 2011, Science, 332, 1396
Belton, M. J. S. 2010, Icarus, 210, 881
Belton, M. J. S. 2014, Icarus, 231, 168
Belton, M. J. S. 2015, Icarus, 245, 87
Capria, M. T., Coradini, A., & De Sanctis, M. C. 2003, Advances in Space Research, 31, 2543
Combi, M. R., Tenishev, V. M., Rubin, M., Fougere, N., & Gombosi, T. I. 2012, ApJ, 749, 29
Enzian, A., Cabot, H., & Klinger, J. 1997, A&A, 319, 995
Farnham, T. L., Besse, S., Feaga, L. M., et al. 2011, in Lunar and Planetary Science Conference, 2160
Feaga, L. M., Sunshine, J. M., Groussin, O., et al. 2011, in Lunar and Planetary Science Conference, 2461

Fulle, M., Marzari, F., Della Corte, V., et al. 2016, ApJ, 821, 19
Gicquel, A., Rose, M., Vincent, J. B., et al. 2017, MNRAS, 469, S178
Gronkowski, P., & Wesołowski, M. 2015a, MNRAS, 451, 3068
Gronkowski, P., & Wesołowski, M. 2015b, Astronomische Nachrichten, 336, 362
Gronkowski, P., & Wesołowski, M. 2017, Astronomische Nachrichten, 338, 385
Groussin, O., Jorda, L., Auger, A. T., et al. 2015, A&A, 583, A32
Hermalyn, B., Schultz, P. H., Farnham, T. L., Bodewits, D., & A'Hearn, M. F. 2011, in Lunar and Planetary Science Conference, 2676
Ipatov, S. I. 2012, MNRAS, 423, 3474
Ipatov, S. I., & A'Hearn, M. F. 2011, MNRAS, 414, 76
Jorda, L., Gaskell, R., Capanna, C., et al. 2016, Icarus, 277, 257
Keller, H. U. 1990, in Physics and Chemistry of Comets, 13
Kopp, G., & Lean, J. L. 2011, Geophys. Res. Lett., 38, L01706
Kossacki, K. J., & Szutowicz, S. 2013, Icarus, 225, 111
Leliwa-Kopystynski, J. 2018, Icarus, 302, 266
Levison, H. F., & Duncan, M. J. 1994, Icarus, 108, 18
Lisse, C. M., Fernandez, Y. R., Reach, W. T., et al. 2009, PASP, 121, 968
Marboeuf, U., Schmitt, B., Petit, J. M., Mousis, O., & Fray, N. 2012, A&A, 542, A82
Pajola, M., Höfner, S., Vincent, J. B., et al. 2017, Nature Astronomy, 1, 0092
Preusker, F., Scholten, F., Matz, K. D., et al. 2015, A&A, 583, A33
Prialnik, D., 2006. What Makes Comets Active? Asteroids, Comets, Meteors, Proceedings of the 229th Symposium of the International Astronomical Union (Cambridge Univ. Press), 153
Schultz, P. H., Hermalyn, B., Bruck, M., et al. 2011, in Lunar and Planetary Science Conference, 2382
Sierks, H., Barbieri, C., Lamy, P. L., et al. 2015, Science, 347, aaa1044
Skorov, Y. V., Rezac, L., Hartogh, P., & Keller, H. U. 2017, A&A, 600, A142
Steckloff, J., & Melosh, H. J. 2016, in AAS/Division for Planetary Sciences Meeting Abstracts, 48, 206.06
Sunshine, J. M., Feaga, L. M., Groussin, O., et al. 2011, in Lunar and Planetary Science Conference, 2292
Thomas, P. C., A'Hearn, M. F., Veverka, J., et al. 2013, Icarus, 222, 550
Tubiana, C., Snodgrass, C., Bertini, I., et al. 2015, A&A, 573, A62
Vincent, J.-B., Bodewits, D., Besse, S., et al. 2015, Nature, 523, 63
Wesołowski, M., & Gronkowski, P. 2018a, New Astron., 62, 55
Wesołowski, M., & Gronkowski, P. 2018b, Earth Moon and Planets, 121, 105
Wesołowski, M., Gronkowski, P., & Tralle, I. 2019, MNRAS, 484, 2309
Wesołowski, M. 2020a, Icarus, 351, 113950
Wesołowski, M. 2020b, Journal of Astrophysics and Astronomy, 41, 1
Wesołowski, M., Gronkowski, P., & Tralle, I. 2020a, Icarus, 352, 114005
Wesołowski, M., Gronkowski, P., & Tralle, I. 2020b, Planet. Space Sci., 184, 104867
Wesołowski, M., Gronkowski, P., & Tralle, I. 2020c, Icarus, 338, 113546
Wesołowski, M. 2021a, New Astron., 89, 101626
Wesołowski, M. 2021b, MNRAS, 505, 3525
Wesołowski, M. 2021c, RAA (Research in Astronomy and Astrophysics), 21, 069
Wesołowski, M. 2021d, Icarus, 357, 114116
Yelle, R. V., Soderblom, L. A., & Jokipii, J. R. 2004, Icarus, 167, 30